BIOMOLECULES & THERAPEUTICS

Original Article
Biomol Ther 30(5), 427-434 (2022)

Abiraterone Acetate Attenuates SARS-CoV-2 Replication by Interfering with the Structural Nucleocapsid Protein

Jinsoo Kim[1,†], Seok Young Hwang[2,†], Dongbum Kim[3,†], Minyoung Kim[1], Kyeongbin Baek[1], Mijeong Kang[1], Seungchan An[2], Junpyo Gong[2], Sangkyu Park[4], Mahmoud Kandeel[5,6], Younghee Lee[4], Minsoo Noh[2,*] and Hyung-Joo Kwon[1,3,*]

[1]Department of Microbiology, College of Medicine, Hallym University, Chuncheon 24252,
[2]College of Pharmacy, Natural Products Research Institute, Seoul National University, Seoul 08826,
[3]Institute of Medical Science, College of Medicine, Hallym University, Chuncheon 24252,
[4]Department of Biochemistry, College of Natural Sciences, Chungbuk National University, Cheongju 28644, Republic of Korea
[5]Department of Biomedical Sciences, College of Veterinary Medicine, King Faisal University, Al-hofuf 31982, Saudi Arabia
[6]Department of Pharmacology, Faculty of Veterinary Medicine, Kafrelshikh University, Kafrelshikh 33516, Egypt

Abstract

The drug repurposing strategy has been applied to the development of emergency COVID-19 therapeutic medicines. Current drug repurposing approaches have been directed against RNA polymerases and viral proteases. Recently, we found that the inhibition of the interaction between the SARS-CoV-2 structural nucleocapsid (N) and spike (S) proteins decreased viral replication. In this study, drug repurposing candidates were screened by *in silico* molecular docking simulation with the SARS-CoV-2 structural N protein. In the ChEMBL database, 1994 FDA-approved drugs were selected for the *in silico* virtual screening against the N terminal domain (NTD) of the SARS-CoV-2 N protein. The tyrosine 109 residue in the NTD of the N protein was used as the center of the ligand binding grid for the docking simulation. In plaque forming assays performed with SARS-CoV-2 infected Vero E6 cells, atovaquone, abiraterone acetate, and digoxin exhibited a tendency to reduce the size of the viral plagues without affecting the plaque numbers. Abiraterone acetate significantly decreased the accumulation of viral particles in the cell culture supernatants in a concentration-dependent manner. In addition, abiraterone acetate significantly decreased the production of N protein and S protein in the SARS-CoV-2-infected Vero E6 cells. In conclusion, abiraterone acetate has therapeutic potential to inhibit the viral replication of SARS-CoV-2.

Key Words: Abiraterone acetate, Docking simulation, Drug repurposing, Nucleocapsid protein, SARS-CoV-2, Virtual screening

INTRODUCTION

Since infection with severe acute respiratory syndrome CoV-2 (SARS-CoV-2) was first reported in Wuhan City, China in December 2019 (Wu *et al*., 2020; Zhou *et al*., 2020a), the pandemic coronavirus disease 2019 (COVID-19) has caused serious challenges for the public health and medical systems worldwide (https://covid19.who.int/). SARS-CoV-2 is an enveloped virus with a plus-stranded RNA genome (varies from 29.8 kb to 29.9 kb) and belongs to lineage B beta-coronaviruses (Khailany *et al*., 2020). SARS-CoV-2 maintains its structure with four major structural protein complexes: spike (S) glycoprotein, nucleocapsid (N) phosphoprotein, membrane (M) glycoprotein and small envelope (E) glycoprotein (Satarker and Nampoothiri, 2020). It is known that angiotensin-converting enzyme 2 (ACE2) is a receptor for SARS-CoV-2 S protein for mediating viral attachment/membrane fusion and that transmembrane protease serine 2 (TMPRSS2) contributes to viral entry into host cells (Datta *et al*., 2020; Matsuyama *et al*., 2020; Zeidler and Karpinski 2020). In this regard, the therapeutic strategy against SARS-CoV-2 infection targeting the entry process is directed towards the development of neu-

Open Access **https://doi.org/10.4062/biomolther.2022.037**

Received Mar 13, 2022 **Revised** Apr 1, 2022 **Accepted** Apr 14, 2022
Published Online May 13, 2022

***Corresponding Authors**
E-mail: hjookwon@hallym.ac.kr (Kwon HJ), minsoonoh@snu.ac.kr (Noh M)
Tel: +82-33-248-2635 (Kwon HJ), +82-02-880-2481 (Noh M)
Fax: +82-33-241-3640 (Kwon HJ), +82-02-880-2482 (Noh M)
[†]The first three authors contributed equally to this work.

tralizing antibodies, fusion inhibitors, and protease inhibitors (Hoffmann *et al*., 2020; Jiang *et al*., 2020; Kandeel *et al*., 2021).

The N protein is essential to the viral RNA packaging and modulation of cellular responses as a multifunctional protein (Perdikari *et al*., 2020). The large RNA genome of SARS-CoV-2 is associated with the N protein to form a helical nucleocapsid (Perdikari *et al*., 2020). The N protein consists of three segments containing two structural domains: the N-terminal domain (NTD), C-terminal domain (CTD), and an intrinsically disordered central Ser/Arg (SR)-rich linker (LKR) (Fig. 1). The NTD of the SARS-CoV-2 N protein interacts with the viral RNA by a hydrogen-bond-forming moiety at the base recognition site. Unlike the NTD of the human coronavirus OC43 (HCoV-OC43) N protein, the NTD of the SARS-CoV-2 N protein has a unique structure that evades steric hindrance at the binding site for a branching phosphate group to maintain a high affinity with the RNA genome (Kang *et al*., 2020). The CTD of the SARS-CoV-2 N protein forms a dimer and has a higher affinity for the first seven ribonucleotides of the SARS-CoV-2 genome compared to previously known affinities of N protein CTDs of other coronaviruses to longer ssRNA or ssDNA (Zhou *et al*., 2020b; Zinzula *et al*., 2020). Recently, we reported a direct interaction between the S and N proteins of MERS-CoV and SARS-CoV-2. The CTD of the S protein interacts with the N protein in MERS-CoV-infected, SARS-CoV-2-infected cells (Kim *et al*., 2021b; Park *et al*., 2021b) and HCoV-OC43-infected cells (Kim *et al*., 2022). Taken together, the N protein of SARS-CoV-2 has gained attention as a target to inhibit the replication of SARS-CoV-2.

Drug repurposing is one of the effective strategies when the development of novel therapeutics is emergent, especially in a pandemic situation. The SARS-CoV-2 N protein is an RNA-binding protein which is essential for both viral RNA replication and viral RNA genome packaging by forming helical ribonucleoproteins (Wu *et al*., 2020). In this study, the drug repurposing strategy was applied to screen therapeutic drugs to inhibit the interaction between the NTD of the SARS-CoV2 N protein and the SARS-CoV-2 genomic RNA by computational docking simulation. The anti-viral activity of the drug repurposing candidates was evaluated with plaque reduction assays using SARS-CoV-2 infected cells.

MATERIALS AND METHODS

Computational docking simulation of the SARS-CoV-2 N protein NTD

The protein structures for the molecular docking simulation were obtained from the Research Collaboratory for Structural Bioinformatics Protein Database (RCSB PDB). PDB entry codes for the NTD of the SARS-CoV2 N protein were 6M3M, 6VYO, 6WKP, and 7CDZ. The assembly modeling for the protein structure prediction with AlphaFold was performed by the web-based server exploiting ColabFold (Jumper *et al*., 2021). For the docking simulation, monomeric forms were isolated from multimeric NTD structures. The monomeric NTD structure was constructed based on the public cryoelectron-tomography model of SARS-CoV-2 ribonucleoproteins (EMD-30429) composed of five N protein dimers, each fitted into head-to-tail reverse L-shaped densities (Yao *et al*., 2020). All monomers were further processed for the docking simulation using the PyMol software (Schrödinger, LLC, New York, NY, USA) and MGLTools (The Scripps Research Institute, La Jolla, CA, USA). The chemical library for the US FDA-approved drugs was constructed as SMILES strings from the ChEMBL Database (https://www.ebi.ac.uk/chembl/) using selection filters to search for phase 3 approved and phase 4 drugs. Constructed SMILES strings were further processed to remove metals and inorganic components in the drugs. After excluding duplicated compounds, 1994 SMILES strings were obtained for the dock-

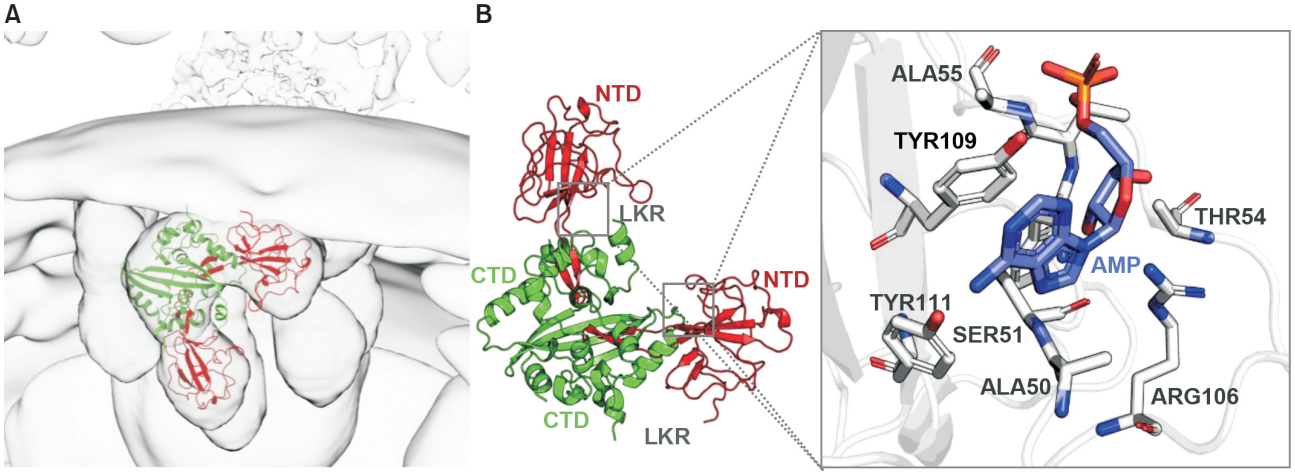

Fig. 1. The ligand binding site of SARS-CoV-2 N protein for the computational docking simulation. (A) The assembly model of the SARS-CoV-2 N protein dimer structure is shown within the viral ribonucleoprotein based on the public cryoelectron tomography model of SARS-CoV-2 (EMD-30429, EMD-30430). (B) The three domains of the N protein dimer constructed by AlphaFold are shown: N-terminal domain (NTD) in red, C-terminal domain (CTD) in green, and an intrinsically disordered central Ser/Arg (SR)-rich linker (LKR) in grey. The ligand binding site of the NTD was defined as a 30 Å sized grid box (shown as gray box) centered on the average centroid of the known RNA binding site of NTD monomer structures. TYR109 residue was located near the center of the grid box and marked as magenta. The interaction model of AMP (blue) and the TYR109 residue of the N protein NTD. The base of AMP was shown to interact via $\pi-\pi$ stacking interaction with the TYR109 residue in the docking simulation. All 3D molecular graphics were conducted using the PyMOL software and UCSC Chimera X.

ing simulations with the N protein NTD monomeric structures. SMILES strings were converted into the three-dimensional (3D) PDB file format for the docking simulations using the OpenBabel software and MGLTools. The molecular modeling simulation was performed using Autodock Vina version 1.1.2 (The Scripps Research Institute). Free energy-minimized docking simulations were performed, and ligand-binding modes were visualized using PyMOL and BIOVIA Discovery Studio (Dassault Systèmes, Velizu-Villacoublay, France).

Cell culture and virus amplification

African green monkey kidney Vero E6 cells and human airway epithelial Calu-3 cells were obtained from the Korean Cell Line Bank (Seoul, Korea). Vero E6 cells and Calu-3 cells were grown in Dulbecco's modified Eagle's medium (DMEM, Thermo Fisher Scientific, Waltham, MA, USA) containing 10% fetal bovine serum (FBS, Thermo Fisher Scientific), 25 mM HEPES, 100 U/mL penicillin, and 100 μg/mL streptomycin in a 5% CO_2 incubator at 37°C. SARS-CoV-2 (hCoV-19/South Korea/KCDC03/2020, NCCP43326) was provided by the National Culture Collection for Pathogens (Osong, Korea). The virus amplification was performed as described elsewhere (Park *et al*., 2019; Kandeel *et al*., 2020). To amplify the virus, 2×10^5 Vero E6 cells (6-well plates, Corning, NY, USA) were cultured in a CO_2 incubator overnight. The 6-well plates were washed with phosphate-buffered saline (PBS), and SARS-CoV-2 in PBS at a MOI of 0.01 was inoculated into each well. Then, the cells were incubated for 1 h with shaking at 15-20 min intervals in a CO_2 incubator. After infection, the suspensions were removed, and DMEM containing 2% FBS (2 mL) was added to each well, and the plates were incubated at 37°C in a CO_2 incubator. After 3 days of cultivation, the cell culture supernatants were harvested, and cell debris was removed by centrifugation at 2,000 rpm for 10 min at 4°C. The virus titer was quantified by plaque assay, and aliquots (5×10^6 plaque forming unit (pfu)/mL) of the virus were stored at –70°C. SARS-CoV-2 amplification and cell culture procedures were performed according to biosafety level 3 (BSL-3) conditions in the Hallym Clinical and Translational Science Institute in accordance with the recommendation of the Institutional Biosafety Committee of Hallym University (Chuncheon, Korea).

Virus quantification

SARS-CoV-2 quantification was performed as described elsewhere (Kim *et al*., 2021a; Park *et al*. 2021a). First, 7×10^5 cells/well of Vero E6 cells were cultured in 6-well plates overnight in 5% CO_2 incubator. Then, the cells were washed with PBS and inoculated with 10-fold serial dilutions of SARS-CoV-2. After a 1 h incubation with shaking at 20 min intervals in a CO_2 incubator, suspensions were removed, and the wells were overlaid with 3 mL DMEM/F12 medium (Thermo Fisher Scientific) containing 2% Oxoid agar and N-*p*-Tosyl-L-phenylalanine chloromethyl ketone (TPCK, 1 μg/mL)-treated trypsin (Sigma-Aldrich, Saint Louis, MO, USA). The plates were incubated in a CO_2 incubator for 72 h at 37°C and then stained with 0.1% crystal violet for 1 h to evaluate plaque formation.

Plaque reduction assay

First, 7×10^5 Vero E6 cells/well were plated on six-well plates for 12 h. Then, SARS-CoV-2 (200 pfu/well) was mixed with each chemical at a final concentration of 10 μM or 1 μM, and Vero E6 cells in each well were treated with the mixtures. After a 1 h incubation with shaking at 20 min intervals in a CO_2 incubator, the supernatant was removed, and the wells were overlaid with 3 mL DMEM/F12 medium (Thermo Fisher Scientific) containing 2% Oxoid agar and TPCK (1 μg/mL)-treated trypsin (Sigma-Aldrich). Finally, 72 h after infection, the plaques formed in each wells were observed with crystal violet satining.

Investigation of SARS-CoV-2 replication in the presence of the chemicals

Vero E6 cells (5×10^4 cells/well 6-well plates) were cultured overnight. The cells were infected with SARS-CoV-2 in PBS (0.1 MOI) for 1 h with shaking at 20 min intervals in a CO_2 incubator at 37°C, and then, 2 mL of DMEM containing 2% FBS were added to each well. After a 3 h incubation in a CO_2 incubator at 37°C, the cells were treated with 0.1% DMSO, atovaquone (Sigma-Aldrich), abiraterone acetate (Sigma-Aldrich), digoxin (Sigma-Aldrich), or β-Estradiol 3-benzoate (Sigma-Aldrich) in a dose-dependent manner, and the plates were incubated for an additional 48 h. Supernatants of the virus-infected cells were collected, and virus replication was quantified using the plaque formation assay.

Cell viability assay

Vero E6 cells (1×10^3 cells/well) were plated onto 96-well plates in DMEM containing 10% FBS for 12 h. Then, the cells were incubated with atovaquone, abiraterone acetate or digoxin at the indicated concentrations for 48 h in DMEM containing 2% FBS. The cells were then treated with 10 μL Cell Counting Kit-8 (CCK-8) solution (Dojindo Molecular Technologies, Rockville, MD, USA) for 2 h at 37°C. Soluble formazan was measured by absorbance at 450 nm using a microplate reader (Thermo Fisher Scientific, Ratastie, Finland) as described elsewhere (Maharjan *et al*., 2021).

Confocal images

The effects of the chemicals on the expression of the N protein and S protein in SARS-CoV-2-infected cells were investigated by indirect immunofluorescence and confocal microscopy. Vero E6 cells were plated on coverslips in 12-well plates overnight and then infected with SARS-CoV-2 (0.1 MOI) in PBS with shaking at 15-20 min intervals in a CO_2 incubator for 1 h at 37°C. After washing with PBS, the cells were cultured in 2 mL of DMEM containing 2% FBS for a 3 h incubation at 37°C, and then, the cells were treated with 0.1% DMSO, abiraterone acetate (10 μM) or atovaquone (10 μM). After a 48 h incubation in a CO_2 incubator, the cells were fixed with 4% paraformaldehyde in PBS, permeabilized with 0.1% Triton X-100, and then blocked with 3% BSA. The permeabilized cells were incubated with rabbit anti-SARS-CoV-2 Spike protein polyclonal antibody (anti-SARS-CoV-2 S Ab, Cat. No. 40592-T62, Sino Biological, Vienna, Austria) or mouse anti-SARS-CoV-2 N protein monoclonal antibody (anti-SARS-CoV-2 S mAb, Cat. No. 40143-MM05, Sino Biological) for 2 h. The cells were then washed with PBST containing 1% BSA and incubated with Alexa Fluor 488-conjugated secondary antibody (Thermo Fisher Scientific) for 1 h. The nuclei were stained with Hoechst 33258. The slides were examined using a Carl Zeiss LSM710 microscope (Carl Zeiss, Oberkochen, Germany).

Statistical analysis

Results are shown as the mean ± standard deviation. Differences between the samples were analyzed using an unpaired, 2-tailed nonparametric t-test of significance (Instat; GraphPad Inc., San Diego, CA, USA). *p*-values<0.05 were considered statistically significant.

RESULTS

Docking simulation for targeting the NTD of the SARS-CoV-2 N protein

The NTD of the SARS-CoV-2 N protein directly binds to RNA molecules by stacking interactions between aromatic amino acids and nucleobases (Kang *et al*., 2020). For the molecular docking simulation, the putative ligand binding sites of four PDB N protein NTD structures, 6M3M, 6VYO, 6WKP, and 7CDZ, were defined as a 30 $Å^3$ size grid box centered on tyrosine (TYR) residue 109 which is the important residue for the RNA binding affinity of SARS-CoV-2 N proteins (Kang *et al*., 2020) (Fig. 1B). In this study, the drug repurposing library was constructed as SMILES strings from the US FDA-approved drugs in the ChEMBL Database. The average binding free energies of the repurposed drug candidates to the energy-minimized docking models for the four PDB NTD structures were calculated and used to prioritize the compounds for biological analysis. In addition, the qualitative selection criteria were used for filtering false positive compounds out in the experimental validation analysis by considering the interaction with the TYR109 residue of the SARS-CoV-2 N protein. After removing the compounds lacking an interaction with TYR109, the US FDA-approved drugs in the repurposing library were listed by rank based on the averaged free energy value (Table 1, Supplementary Table 1). Next, extensive literature studies for the top 100 ranked compounds were performed to set the priorities for evaluating their anti-viral activity against SARS-CoV-2. Through this process, several compounds were excluded due to the well-established antiviral activities found in prior reports or the therapeutic unsuitability of the compounds. For instance, proscillaridin was excluded because of the prior reports for its antiviral activity (Jeon *et al*., 2020). In addition, venetoclax was excluded because it had been reported that it could worsen the symptoms of COVID-19 in chronic lymphocytic leukemia (CLL) patients (Fürstenau *et al*., 2020).

Screening by the viral plaque reduction assay

The anti-viral activities of twelve FDA-approved drug candidates were evaluated by the plaque reduction assay with SARS-CoV-2. Each FDA-approved drug was mixed with SARS-CoV-2 (200 pfu) at a final concentration of 1 or 10 μM, and then, Vero E6 cells were treated with the mixture. In the plaque reduction assay results, no chemicals significantly reduced the number of plaques. However, three drugs, atovaquone, abiraterone acetate, and digoxin, tended to reduce the size of the SARS-CoV-2 viral plaques in the preliminary screening assays (Fig. 2A-2C). In the best optimized docking models, atovaquone, abiraterone acetate, and digoxin interacted with the TYR109 residue of the N protein NTD (Fig. 3). In the energy-optimized model, atovaquone interacted with the TYR109 residue via π-π stacking interactions whereas abi-

Table 1. Analysis of N-protein docking results and prioritized compound sets

Compounds	Binding free energy (kcal/mol)				
	6M3M	6VYO	6WKP	7CDZ	average
Ergotamine	–8.1	–7.1	–7.4	–7.8	–7.6 ± 0.4
Abiraterone	–7.1	–7.4	–6.9	–7.3	–7.2 ± 0.2
Digoxin	–7.1	–7.2	–7.1	–7.2	–7.2 ± 0.1
Lumacaftor	–7	–7.2	–7.2	–7.1	–7.1 ± 0.1
Eltrombopag	–7.5	–7.4	–6.6	–7	–7.1 ± 0.4
Abiraterone acetate	–7	–7.4	–6.8	–7.3	–7.1 ± 0.3
Proscillaridin	–7.4	–7	–6.8	–7.2	–7.1 ± 0.3
Atovaquone	–6.9	–7.4	–6.8	–6.9	–7.0 ± 0.3
Olaparib	–7.2	–6.5	–6.9	–7	–6.9 ± 0.3
Fluspirilene	–7.1	–7	–6.7	–6.4	–6.8 ± 0.3
Difenoxin	–6.8	–6.6	–6.6	–6.9	–6.7 ± 0.2
Quinestrol	–6.9	–7.3	–6.2	–6.5	–6.7 ± 0.5
Norethynodrel	–6.8	–7	–6.2	–6.8	–6.7 ± 0.3
Venetoclax	–7.3	–6.3	–6.5	–6.5	–6.7 ± 0.4

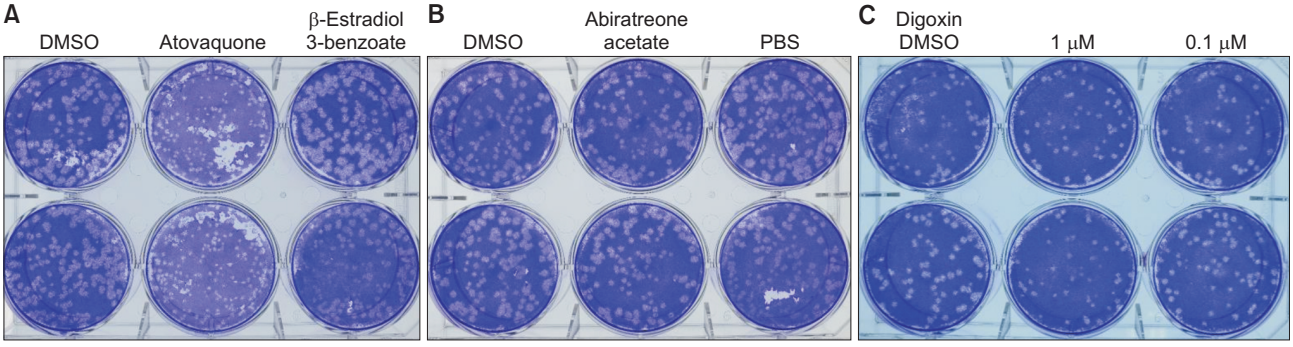

Fig. 2. Screening of the FDA-approved drugs against SARS-CoV-2 infection in Vero E6 cells. The plaque reduction assay was performed with 12 FDA-approved drugs. SARS-CoV-2 was mixed with 10 μM or the indicated concentrations of each compound, and then, the mixture was used to infect Vero E6 cells for 1 h. The supernatant was removed and overlaid with 3 mL DMEM/F12 medium containing 2% Oxoid agar and TPCK (1 μg/mL)-treated trypsin. After a 72 h infection, the plaques were observed by staining with crystal violet. These data show only 5 representatives of the 18 FDA-approved drugs. (A) Effect of atovaquone (10 μM) and β-estradiol 3-benzoate (10 μM) on SARS-CoV-2 infection. (B) Effect of abiraterone acetate (10 μM) on SARS-CoV-2 infection. (C) Effect of digoxin on SARS-CoV-2 infection at each concentration.

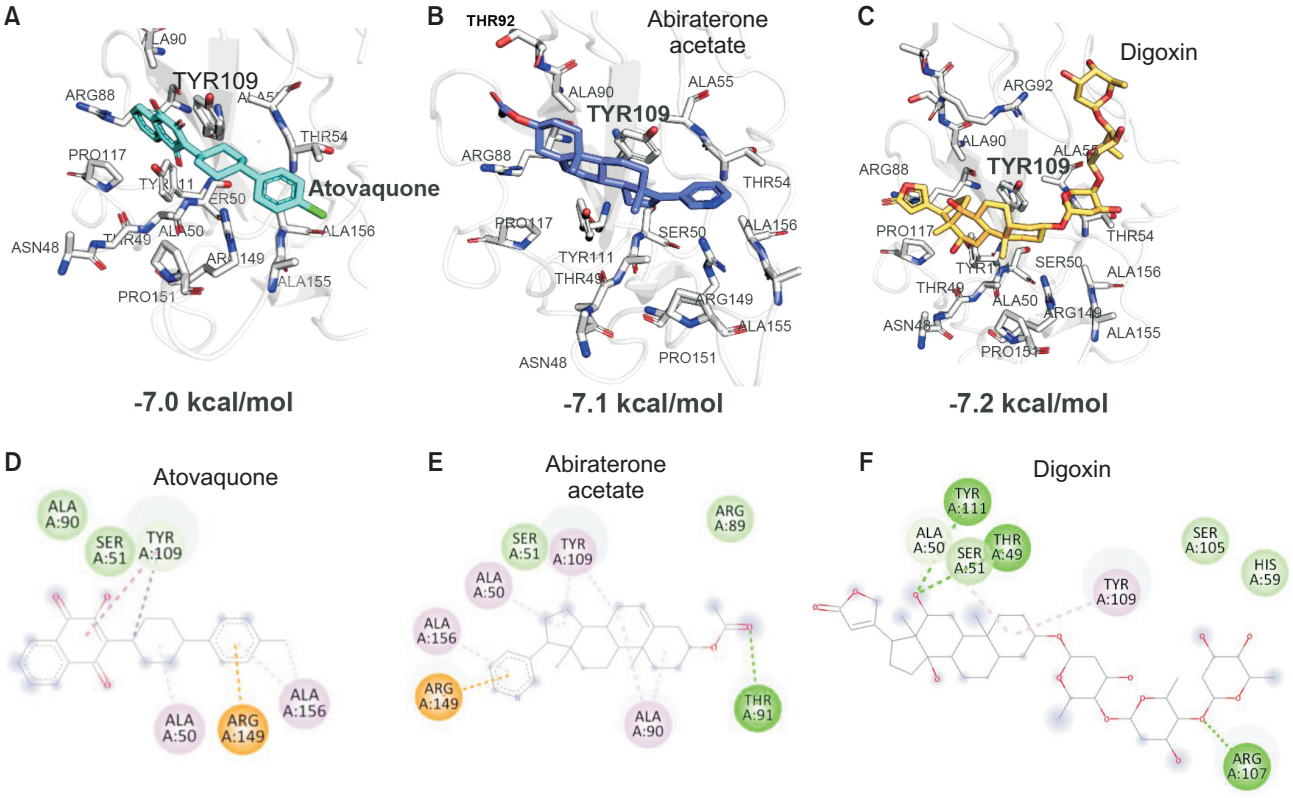

Fig. 3. The binding modes of drugs affecting the viral plaque size. The optimum binding models of atovaquone (A), abiraterone acetate (B), and digoxin (C) were constructed with the SARS-CoV-2 N protein NTD monomer structure (PDB ID: 6M3M). Protein residues were numbered based on the Uniprot sequence number (Uniprot ID: P0DTC9). The detailed interaction models of atovaquone (D), abiraterone acetate (E) and digoxin (F) were provided in 2D representation. 2D molecular graphics were conducted using BIOVIA Discovery Studio Visualizer.

raterone acetate and digoxin bound to the TYR109 residue with π-alkyl interactions. Notably, abiraterone acetate formed an additional hydrogen bond with the THR91 residue of the NTD and was surrounded by the binding pocket residues including TYR109 (Fig. 3E).

After the COVID-19 pandemic, many drug reposition studies have been reported for FDA-approved drugs. Although abiraterone acetate (Yuan *et al*., 2020) and digoxin (Cho *et al*., 2020) along with atovaquone (Farag *et al*., 2020) were evaluated as SARS-CoV-2 antivirals *in vitro*, the effects of abiraterone acetate and digoxin were controversial, especially in reducing the number of plaques. The plaque reduction assay is cost-effective for screening purposes, but it has a limitation in determining the anti-viral activity of chemicals targeting viral structural proteins like SARS-CoV-2 N proteins because anti-replicative anti-viral drugs may not affect the entry of the virus into cells.

Investigation of the antiviral activity by counting virus particle numbers in the cell culture supernatant

To overcome the limitation of screening for SARS-CoV-2 replication inhibitors by the plaque reduction assay, quantitative analysis was performed by measuring the number of virus particles produced in culture supernatants using the plaque assay. When Vero E6 cells were infected with a 0.1 MOI of SARS-CoV-2 and then treated with the drug candidates for 48 h, atovaquone had no effect on the viral secretion into the supernatants (Fig. 4A). Notably, abiraterone acetate reduced the virus particles in the culture supernatants in a concentration-dependent manner (Fig. 4B). Specifically, the plaque formation was significantly reduced by above two logarithmic scales in the presence of 10 μM of abiraterone acetate. Digoxin also significantly reduced the accumulation of virus particles in the culture supernatants (Fig. 4C). To exclude a non-specific effect of the drugs in cell-based assays, the cell viability was evaluated with CCK-8-based cytotoxicity assays. The cell viability of the Vero E6 cells was unaffected when exposed to up to 50 μM of atovaquone and abiraterone acetate (Fig. 4D). However, digoxin exhibited a significant cytotoxicity against Vero E6 cells even at much lower concentrations. Therefore, the significant inhibitory effect of abiraterone acetate on virus particle accumulation in the cell culture supernatants was not associated with non-specific cytotoxicity.

Effects of the drugs on SARS-CoV-2 N protein and S protein production

In the measurement of the live virus in the culture supernatant, abiraterone acetate exhibited a concentration-dependent inhibitory activity (Fig. 4). To investigate the inhibitory mechanism in detail, we examined the effects of abiraterone acetate on SARS-CoV-2 N protein and S protein expression in Vero E6 cells. Vero E6 cells were infected with SARS-CoV-2 (0.1

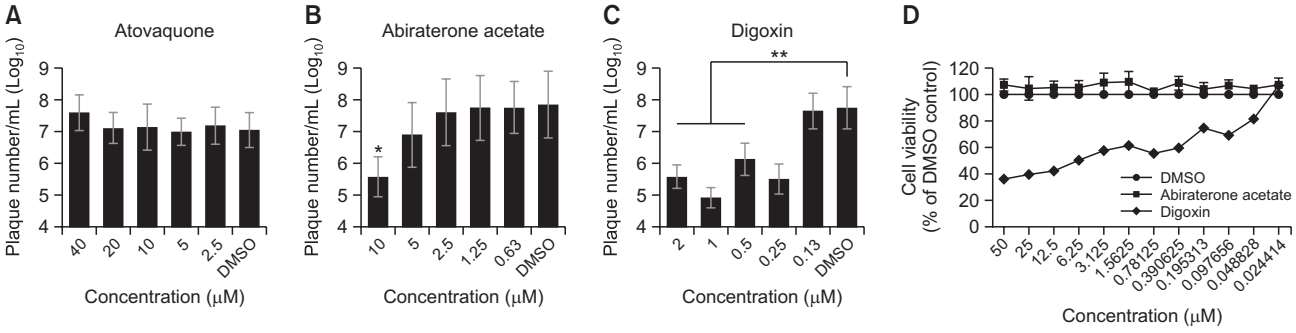

Fig. 4. Effect of the FDA-approved drugs on the replication of SARS-CoV-2 and cell viability. (A-C) Vero E6 cells were infected with a 0.1 MOI of SARS-CoV-2 in 6-well plates and then treated with 0.1% DMSO, atovaquone (A), abiraterone acetate (B) or digoxin (C) in a dose-dependent manner at 3 h after virus infection. Supernatants of the virus-infected cell cultures were collected at 48 h after virus infection. Viral replication was quantified by plaque formation assay. *p<0.05, **p<0.01. (D) Effect of the FDA-approved drugs on the cell viability of Vero E6 cells. Vero E6 cells were cultured in DMEM medium containing 2% FBS with the indicated concentrations of each FDA-approved drug for 48 h. The cells were incubated with CCK-8 solution, and then, soluble formazan was measured using a microplate reader.

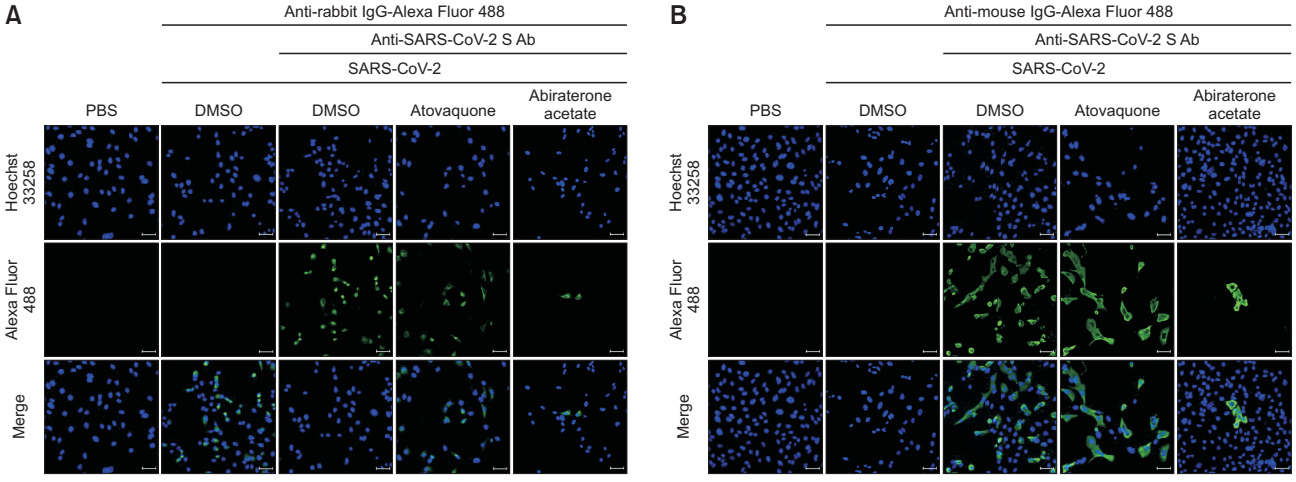

Fig. 5. Effects of the FDA-approved drugs on the SARS-CoV-2 N protein and S protein production. Vero E6 cells were infected with a 0.1 MOI of SARS-CoV-2 in 12-well plates and then treated with 0.1% DMSO, atovaquone (10 μM) or abiraterone acetate (10 μM) at 3 h after virus infection. The cells were cultured for 48 h in DMEM media containing 2% FBS. Confocal images were analyzed using a Carl Zeiss LSM710 microscope after staining with anti-SARS-CoV S Ab (A) or anti-SARS-CoV N mAb (B) and then Alexa Fluor 488-conjugated secondary antibody. Scale bar, 20 μm.

MOI) and then treated with atovaquone and abiraterone acetate. The immunofluorescence data of the confocal images showed that abiraterone acetate significantly reduced the expression of the S and N proteins in the SARS-CoV-2-infected Vero E6 cells (Fig. 5). However, atovaquone did not affect the expression of the S and N proteins in the infected cells (Fig. 5). Conclusively, abiraterone acetate has a therapeutic potential to inhibit the viral particle formation of SARS-CoV-2 by interfering with the interaction between viral RNAs and SARS-CoV-2 structural N proteins.

DISCUSSION

Although people are being currently vaccinated against SARS-CoV-2 in many countries, there is an unmet medical need to find potential therapeutics using drug-repurposing strategies. Large scale screening has been performed to find FDA-approved drugs that inhibit SARS-CoV-2 replication (Jeon *et al*., 2020; Liu *et al*., 2020; Riva *et al*., 2020; Weston *et al*., 2020; Yuan *et al*., 2020). Many studies have investigated proteases such as TMPRSS2 (Hoffmann *et al*., 2020), cathepsin B/L (Padmanabhan *et al*., 2020), main protease (M^{pro}) (Sternberg *et al*., 2020) and papain-like protease (PLpro) (Klemm *et al*., 2020) as potential therapeutic targets for the treatment of SARS-CoV-2 infection. Therefore, there have been many published reports concerning protease inhibitors inhibiting SARS-CoV-2 replication screened from FDA-approved drugs. Currently, drug-repurposing studies targeting viral structual proteins are less available in the literature.

The N protein of coronavirus is essential to the virus assembly through direct interaction with the viral RNA. Therefore, chemicals interfering with the interaction between the viral RNA and the N protein have therapeutic potential against SARS-CoV-2 infection by directly affecting viral replication. In this study, we screened candidate chemicals capable of inter-

acting with N proteins from FDA-approved drugs through *in silico* docking analyses with four PDB N protein NTD structures, 6M3M, 6VYO, 6WKP, and 7CDZ. The conventional *in silico* screening is based on the energy-minimized docking models of test chemicals (Forli *et al*., 2016). To select candidate drugs, the interaction between the TYR109 residue of the N protein and a test chemical was introduced as an additional selection filter. We tested 12 FDA-approved drugs in the SARS-CoV-2 plaque reduction assay to validate the *in silico* screening result. However, none of the 12 candidate drugs reduced the number of the SARS-CoV-2 viral plagues. Atovaquone, abiraterone acetate, and digoxin were likely to reduce the size of the viral plagues. This result can be explained in that the drug targeting the SARS-CoV-2 structural N protein cannot inhibit the cellular entry of SARS-CoV-2 but can inhibit viral replication. For the development of an optimal method to evaluate drug candidates against structural proteins essential in viral replication, we treated the cells with the candidate drugs for 3 h after SARS-CoV-2 infection and measured the production of viral progeny particles. As a result, we confirmed that abiraterone acetate significantly inhibited the amount of virus progeny in cell culture supernatants. However, atovaquone and digoxin had no effect on the viral particle accumulation in the supernatants, Notably, it was reported that digoxin significantly inhibited the replication of SARS-CoV-2 (Cho *et al*., 2020). Digoxin is currently being prescribed to manage atrial fibrillation, atrial flutter, and heart failure as an inhibitor of sodium potassium adenosine triphosphatase (Na^+/K^+ ATPase) (Kjeldsen *et al*., 2002). In our study, digoxin exhibited a severe cytotoxicity in SARS-CoV-2-infected Vero E6 cells. Further studies should be directed to resolve the conflicting results to use digoxin as a therapeutic drug against SARS-CoV-2 infection.

The medical use of abiraterone acetate is to treat prostate cancer (Yin and Hu, 2014). Abiraterone acetate is an active metabolite of abiraterone and inhibits cytochrome P450 17A1, also called 17α-hydroxylase, and functions as an antagonist of the androgen receptor (Yin and Hu, 2014). In this regard, it is necessary to check whether the inhibition of CYP17A1 or androgen function contributes to the inhibitory effect of abiraterone acetate on SARS-CoV-2 replication through the inhibition of N protein functions. In conclusion, abiraterone acetate has therapeutic potential by inhibiting viral replication in SARS-CoV-2.

CONFLICT OF INTEREST

The authors declare no financial or commercial conflict of interest.

ACKNOWLEDGMENTS

We thank the National Culture Collection for Pathogens for providing the SARS-CoV-2 (hCoV-19/South Korea/KCDC03/2020, NCCP No. 43326). This research was supported by grants from the National Research Foundation (NRF-2020M3A9I2107294) funded by the Ministry of Science and ICT in the Republic of Korea.

This work was also supported by the Deanship of Scientific Research, Vice Presidency for Graduate Studies and Scientific Research, King Faisal University, Saudi Arabia (Project No. GRANT672).

REFERENCES

Cho, J., Lee, Y. J., Kim, J. H., Kim, S. I., Kim, S. S., Choi, B. S. and Choi, J. H. (2020) Antiviral activity of digoxin and ouabain against SARS-CoV-2 infection and its implication for COVID-19. *Sci. Rep*. **10**, 16200.

Datta, P. K., Liu, F., Fischer, T., Rappaport, J. and Qin, X. (2020) SARS-CoV-2 pandemic and research gaps: understanding SARS-CoV-2 interaction with the ACE2 receptor and implications for therapy. *Theranostics* **10**, 7448-7464.

Farag, A. B., Wang, P., Boys, I. N., Eitson, J. L., Ohlson, M. B., Fan, W., McDougal, M. B., Amed, M. S., Schoggins, J. W. and Sadek, H. A. (2020) Identification of Atovaquone, Ouabain and Mebendazole as FDA approved drugs targeting SARS-CoV-2 (Version 4). *ChemRxiv* doi: 10.26434/chemrxiv.12003930.v4 [Preprint].

Forli, S., Huey, R., Pique, M. E., Sanner, M. F., Goodsell, D. S. and Olson, A. J. (2016) Computational protein–ligand docking and virtual drug screening with the AutoDock suite. *Nature Protoc*. **11**, 905-919.

Fürstenau, M., Langerbeins, P., De Silva, N., Fink, A. M., Robrecht, S., von Tresckow, J., Simon, F., Hohloch, K., Droogendijk, J., van der Klift, M., van der Spek, E., Illmer, T., Schöttker, B., Fischer, K., Wendtner, C. M., Tausch, E., Stilgenbauer, S., Niemann, C. U., Gregor, M., Kater, A. P., Hallek, M. and Eichhorst, B. (2020) COVID-19 among fit patients with CLL treated with venetoclax-based combinations. *Leukemia* **34**, 2225-2229.

Hoffmann, M., Kleine-Weber, H., Schroeder, S., Krüger, N., Herrler, T., Erichsen, S., Schiergens, T. S., Herrler, G., Wu, N. H., Nitsche, A., Müller, M. A., Drosten, C. and Pöhlmann, S. (2020) SARS-CoV-2 cell entry depends on ACE2 and TMPRSS2 and is blocked by a clinically proven protease inhibitor. *Cell* **181**, 271-280.e8.

Jeon, S., Ko, M., Lee, J., Choi, I., Byun, S. Y., Park, S., Shum, D. and Kim, S. (2020) Identification of antiviral drug candidates against SARS-CoV-2 from FDA-approved drugs. *Antimicrob. Agents Chemother*. **64**, e00819-20.

Jiang, S., Hillyer, C. and Du, L. (2020) Neutralizing antibodies against SARS-CoV-2 and other human coronaviruses. *Trends Immunol*. **41**, 355-359.

Jumper, J., Evans, R., Pritzel, A., Green, T., Figurnov, M., Ronneberger, O., Tunyasuvunakool, K., Bates, R., Žídek, A., Potapenko, A., Bridgland, A., Meyer, C., Kohl, S. A. A., Ballard, A. J., Cowie, A., Romera-Paredes, B., Nikolov, S., Jain, R., Adler, J., Back, T., Petersen, S., Reiman, D., Clancy, E., Zielinski, M., Steinegger, M., Pacholska, M., Berghammer, T., Bodenstein, S., Silver, D., Vinyals, O., Senior, A. W., Kavukcuoglu, K., Kohli, P. and Hassabis, D. (2021) Highly accurate protein structure prediction with AlphaFold. *Nature* **596**, 583-589.

Kandeel, M., Yamamoto, M., Al-Taher, A., Watanabe, A., Oh-Hashi, K., Park, B. K., Kwon, H. J., Inoue, J. I. and Al-Nazawi, M. (2020) Small molecule inhibitors of Middle East respiratory syndrome coronavirus fusion by targeting cavities on heptad repeat trimers. *Biomol. Ther. (Seoul)* **28**, 311-319.

Kandeel, M., Yamamoto, M., Tani, H., Kobayashi, A., Gohda, J., Kawaguchi, Y., Park, B. K., Kwon, H. J., Inoue, J. I. and Alkattan, A. (2021) Discovery of new fusion inhibitor peptides against SARS-CoV-2 by targeting the spike S2 subunit. *Biomol. Ther. (Seoul)* **29**, 282-289.

Kang, S., Yang, M., Hong, Z., Zhang, L., Huang, Z., Chen, X., He, S., Zhou, Z., Zhou, Z., Chen, Q., Yan, Y., Zhang, C., Shan, H. and Chen, S. (2020) Crystal structure of SARS-CoV-2 nucleocapsid protein RNA binding domain reveals potential unique drug targeting sites. *Acta Pharm. Sin. B* **10**, 1228-1238.

Khailany, R. A., Safdar, M. and Ozaslan, M. (2020) Genomic characterization of a novel SARS-CoV-2. *Gene Rep*. **19**, 100682.

Kim, D., Maharjan, S., Kim, J., Park, S., Park, J. A., Park, B. K., Lee, Y. and Kwon, H. J. (2021a) MUC1-C influences cell survival in lung adenocarcinoma Calu-3 cells after SARS-CoV-2 infection. *BMB*

Rep. **54**, 425-430.
Kim, D., Kim, J., Park, S., Kim, M., Baek, K., Kang, M., Choi, J. K., Maharjan, S., Akauliya, M., Lee, Y. and Kwon, H. J. (2021b) Production of SARS-CoV-2 N protein-specific monoclonal antibody and its application in an ELISA-based detection system and targeting the interaction between the spike C-terminal domain and N protein. *Front. Microbiol*. **12**, 726231.
Kim, J., Kim, M., Kim, D., Park, S., Kang, M., Baek, K., Choi, J. K., Maharjan, S., Akauliya, M., Lee, Y. and Kwon, H. J. (2022) Targeting the interaction between spike protein and nucleocapsid protein for suppression and detection of human coronavirus OC43. *Front. Immunol*. **13**, 835333.
Kjeldsen, K., Nørgaard, A. and Gheorghiade, M. (2002) Myocardial Na,K-ATPase: the molecular basis for the hemodynamic effect of digoxin therapy in congestive heart failure. *Cardiovasc. Res*. **55**, 710-713.
Klemm, T., Ebert, G., Calleja, D. J., Allison, C. C., Richardson, L. W., Bernardini, J. P., Lu, B. G., Kuchel, N. W., Grohmann, C., Shibata, Y., Gan, Z. Y., Cooney, J. P., Doerflinger, M., Au, A. E., Blackmore, T. R., van der Heden van Noort, G. J., Geurink, P. P., Ovaa, H., Newman, J., Riboldi-Tunnicliffe, A., Czabotar, P. E., Mitchell, J. P., Feltham, R., Lechtenberg, B. C., Lowes, K. N., Dewson, G., Pellegrini, M., Lessene, G. and Komander, D. (2020) Mechanism and inhibition of the papain-like protease, PLpro, of SARS-CoV-2. *EMBO J*. **39**, e106275.
Liu, S., Lien, C. Z., Selvaraj, P. and Wang, T. T. (2020) Evaluation of 19 antiviral drugs against SARS-CoV-2 Infection. *bioRxiv* doi: 10.1101/2020.04.29.067983 [Preprint].
Maharjan, S., Kang, M., Kim, J., Kim, D., Park, S., Kim, M., Baek, K., Lee, Y. and Kwon, H. J. (2021) Apoptosis enhances the replication of human coronavirus OC43. *Viruses* **13**, 2199.
Matsuyama, S., Nao, N., Shirato, K., Kawase, M., Saito, S., Takayama, I., Nagata, N., Sekizuka, T., Katoh, H., Kato, F., Sakata, M., Tahara, M., Kutsuna, S., Ohmagari, N., Kuroda, M., Suzuki, T., Kageyama, T. and Takeda, M. (2020) Enhanced isolation of SARS-CoV-2 by TMPRSS2-expressing cells. *Proc. Natl. Acad. Sci. U.S.A.* **117**, 7001-7003.
Padmanabhan, P., Desikan, R. and Dixit, N. M. (2020) Targeting TMPRSS2 and Cathepsin B/L together may be synergistic against SARS-CoV-2 infection. *PLoS Comput. Biol.* **16**, e1008461.
Park, B. K., Maharjan, S., Lee, S. I., Kim, J., Bae, J. Y., Park, M. S. and Kwon, H. J. (2019) Generation and characterization of a monoclonal antibody against MERS-CoV targeting the spike protein using a synthetic peptide epitope-CpG-DNA-liposome complex. *BMB Rep*. **52**, 397-402.
Park, B. K., Kim, D., Park, S., Maharjan, S., Kim, J., Choi, J. K., Akauliya, M., Lee, Y. and Kwon, H. J. (2021a) Differential signaling and virus production in Calu-3 cells and Vero cells upon SARS-CoV-infection. *Biomol. Ther. (Seoul)* **29**, 273-281.
Park, B. K., Kim, J., Park, S., Kim, D., Kim, M., Baek, K., Bae, J. Y., Park, M. S., Kim, W. K., Lee, Y. and Kwon, H. J. (2021b) MERS-CoV and SARS-CoV-2 replication can be inhibited by targeting the interaction between the viral spike protein and the nucleocapsid protein. *Theranostics* **11**, 3853-3867.
Perdikari, T. M., Murthy, A. C., Ryan, V. H., Watters, S., Naik, M. T. and Fawzi, N. L. (2020) SARS-CoV-2 nucleocapsid protein phase-separates with RNA and with human hnRNPs. *EMBO J*. **39**, e106478.
Riva, L., Yuan, S., Yin, X., Martin-Sancho, L., Matsunaga, N., Burgstaller-Muehlbacher, S., Pache, L., De Jesus, P. P., Hull, M. V., Chang, M., Chan, J. F., Cao, J., Poon, V. K., Herbert, K., Nguyen, T. T., Pu, Y., Nguyen, C., Rubanov, A., Martinez-Sobrido, L., Liu, W. C., Miorin, L., White, K. M., Johnson, J. R., Benner, C., Sun, R., Schultz, P. G., Su, A., Garcia-Sastre, A., Chatterjee, A. K., Yuen, K. Y. and Chanda, S. K. (2020) A large-scale drug repositioning survey for SARS-CoV-2 antivirals. *bioRxiv* doi: 10.1101/2020.04.16.044016 [Preprint].
Satarker, S. and Nampoothiri, M. (2020) Structural proteins in severe acute respiratory syndrome coronavirus-2. *Arch. Med. Res*. **51**, 482-491.
Sternberg, A., McKee, D. L. and Naujokat, C. (2020) Novel drugs targeting the SARS-CoV-2/COVID-19 machinery. *Curr. Top. Med. Chem*. **20**, 1423-1433.
Weston, S., Coleman, C. M., Haupt, R., Logue, J., Matthews, K., Li, Y., Reyes, H. M., Weiss, S. R. and Frieman, M. B. (2020) Broad anti-coronavirus activity of Food and Drug Administration-approved drugs against SARS-CoV-2 *in vitro* and SARS-CoV *in vivo*. *J. Virol.* **94**, e01218-20.
Wu, F., Zhao, S., Yu, B., Chen, Y. M., Wang, W., Song, Z. G., Hum, Y., Tao, Z. W., Tian, J. H., Pei, Y. Y., Yuan, M. L., Zhang, Y. L., Dai, F. H., Liu, Y., Wang, Q. M., Zheng, J. J., Xu, L., Holmes, E. C. and Zhang, Y. Z. (2020) A new coronavirus associated with human respiratory disease in China. *Nature* **579**, 265-269.
Yao, H., Song, Y., Chen, Y., Wu, N., Xu, J., Sun, C., Zhang, J., Weng, T., Zhang, Z., Wu, Z., Cheng, L., Shi, D., Lu, X., Lei, J., Crispin, M., Shi, Y., Li, L. and Li, S. (2020) Molecular architecture of the SARS-CoV-2 virus. *Cell* **183**, 730-738.e13.
Yin, L. and Hu, Q. (2014) CYP17 inhibitors--abiraterone, C17,20-lyase inhibitors and multi-targeting agents. *Nat. Rev. Urol*. **11**, 32-42.
Yuan, S., Chan, J. F. W., Chik, K. K. H., Chan, C. C. Y., Tsang, J. O. L., Liang, R., Cao, J., Tang, K., Chen, L. L., Wen, K., Cai, J. P., Ye, Z. W., Lu, G., Chu, H., Jin, D. Y. and Yuen, K. Y. (2020) Discovery of the FDA-approved drugs bexarotene, cetilistat, diiodohydroxyquinoline, and abiraterone as potential COVID-19 treatments with a robust two-tier screening system. *Pharmacol. Res*. **159**, 104960.
Zeidler, A. and Karpinski, T. M. (2020) SARS-CoV, MERS-CoV, SARS-CoV-2 comparison of three emerging coronaviruses. *Jundishapur J. Microbiol*. **13**, e103744.
Zhou, P., Yang, X. L., Wang, X. G., Hu, B., Zhang, L., Zhang, W., Si, H. R., Zhu, Y., Li, B., Huang, C. L., Chen, H. D., Chen, J., Luo, Y., Guo, H., Jiang, R. D., Liu, M. Q., Chen, Y., Shen, X. R., Wang, X., Zheng, X. S., Zhao, K., Chen, Q. J., Deng, F., Liu, L. L., Yan, B., Zhan, F. X., Wang, Y. Y., Xiao, G. F. and Shi, Z. L. (2020a) A pneumonia outbreak associated with a new coronavirus of probable bat origin. *Nature* **579**, 270-273.
Zhou, R., Zeng, R., von Brunn, A. and Lei, J. (2020b) Structural characterization of the C-terminal domain of SARS-CoV-2 nucleocapsid protein. *Mol. Biomed*. **1**, 2.
Zinzula, L., Basquin, J., Bohn, S., Beck, F., Klumpe, S., Pfeifer, G., Nagy, I., Bracher, A., Hartl, F. U. and Baumeister, W. (2020) High-resolution structure and biophysical characterization of the nucleocapsid phosphoprotein dimerization domain from the Covid-19 severe acute respiratory syndrome coronavirus 2. *Biochem. Biophys. Res. Commun*. **538**, 54-62.